Materials and Corrosion

Stress Corrosion Cracking of Copper in Swollen Bentonite Simulating Nuclear Waste Disposal Environment

Journal:	*Materials and Corrosion*
Manuscript ID	maco.202011878.R1
Wiley - Manuscript type:	Article
Date Submitted by the Author:	n/a
Complete List of Authors:	Fujimoto, Shinji; Osaka University, Div Materials and Manufacturing Sci. Tsuchiya, Hiroaki; Osaka University, Div Materials and Manufacturing Sci. Ogawa, Soma; Osaka University, Div Materials and Manufacturing Sci. Iida, Yoshihisa; Japan Atomic Energy Agency, Nuclear Safety Research Center Taniguchi, Naoki; Japan Atomic Energy Agency, Nuclear Backend Technology Center
Keywords:	spent nuclear fuel waste, SCC, NH₃, tarnish rupture, slow strain rate testing

Stress Corrosion Cracking of Copper in Swollen Bentonite Simulating Nuclear Waste Disposal Environment

Shinji Fujimoto[1], Hiroaki Tsuchiya[1], Soma Ogawa[1], Yoshihisa Iida[2], and Naoki Taniguchi[3]

[1] Division of Materials and Manufacturing Science, Graduate School of Engineering, Osaka University.

[2] Nuclear Safety Research Center, Japan Atomic Energy Agency.

[3] Nuclear Backend Technology Center, Japan Atomic Energy Agency.

Correspondence

Shinji Fujimoto, Division of Materials and Manufacturing Science, Graduate School of Engineering, Osaka University, 2-1 Yamada-oka, Suita, Osaka 565-0871, Japan

E-mail fujimoto@mat.eng.osaka-u.ac.jp

Abstract

The stress corrosion cracking (SCC) of pure copper in bentonite clay was examined using a slow strain rate test (SSRT). The bentonite was swollen with pure water or aqueous solutions containing NH_3 of 5 mM and 10 mM. Thick corrosion films and particulate deposits were formed on the copper surface after the SSRT. Typical tarnish rupture type SCC occurred on pure copper in swollen bentonite with and without NH_3. Crack propagation rate was enhanced by NH_3. It is confirmed that a thick oxide layer was formed on copper during plastic deformation, resulting in tarnish crack type SCC. Many particulate deposits observed on the surface were formed because of the rapid dissolution of Cu^{2+} ions to form porous CuO at local deformed sites, regardless of the SCC occurrence.

KEYWORDS

spent nuclear fuel waste, SCC, NH_3, tarnish rupture

1 INTRODUCTION

Copper has been selected as a candidate overpack material in some countries, including Sweden, Finland, and recently Canada [1]. However, in Japan, carbon steel has been proposed as an overpack material [2, 3]. On the other hand, as the layered structure comprising a carbon steel insert and an outer shell of copper has been proposed, the corrosion behavior of copper has been examined as an alternative overpack material.

The corrosion behavior of copper has been studied in simulated ground water. In particular, the effect of sulfide has been extensively examined because sulfide is the only possible oxidant for copper after oxygen in the system is consumed [4-7]. Furthermore, the effects of bentonite on the corrosion of copper have also been investigated using bentonite clay or solutions containing extracts of swollen bentonite, such as chloride, sulfate, and bicarbonate [8,9]. These studies indicated that the corrosion of copper is not necessarily severe in bentonite clay environments, while the authors of the present study revealed the growth process of corrosion products including oxides and sulfide of copper in the swollen bentonite [10]. Although the corrosion behavior of copper was examined as a candidate for overpack material, the SCC of copper in a simulated geological disposal environment has rarely been studied. A previous investigation by Taniguchi *et al.* on the localized corrosion of pure copper in simulated groundwater containing sulfide reported that copper was subjected to intergranular corrosion at a lower concentration of sulfide, whereas SCC occurred at a higher sulfide concentration [11]. However, the possibility of localized corrosion, including the SCC of copper in bentonite clay, has not been clarified. In the present study, the authors examined the SCC of pure copper in the bentonite swollen with water with or without ammonium ions.

2 EXPERIMENTAL

The material examined was oxygen-free pure copper sheet with a thickness of 1.5 mm. The tensile specimens were cut from the sheet using an electric discharge cutting

machine. The shape of the tensile specimen is shown in Fig.1 (a). Besides, the coupon specimens of 10×10mm^2 were also prepared from the same sheet. The specimens were annealed at 823 K for 1 h under an Ar atmosphere and then cooled in a furnace. After the heat-treatment, the gauge section surface including the tensile specimen edge was dry-polished using SiC papers, and then cleaned with deionized water and acetone, successively in an ultrasonic bath. The surface of the coupon specimen was also prepared similarly. A slow strain rate test (SSRT) was performed at 323 K for the tensile specimen accommodated in an airtight environmental cell filled with a swollen bentonite. A schematic drawing of the environmental cell is depicted in Fig. 1 (b). The swollen bentonite used in the present study was prepared by mixing 5.8 g of bentonite powder (Kunigel-VI, Kunimine Ind., Co., Ltd.) with 50 mL each of deionized water, and ammonia aqueous solutions with the concentrations of 5 mM and 10 mM. The swollen bentonite for the SSRT was prepared in a laboratory atmosphere and used without any deaeration. The tensile specimens were elongated up to a strain of 10% with a strain rate of 1.7×10^{-7} s^{-1}. Immediately after the SSRT termination, the tensile specimen surface was cleaned using pure water to thoroughly remove the swollen bentonite attached to the specimen surface. The surface and cross-sections of the specimens were characterized using scanning electron microscopy (SEM) equipped with an energy dispersive X-ray (EDX) analysis and micro Raman spectroscopy.

3 RESULTS

3.1 Surface characterization

Figure 2 shows SEM images of the specimen surfaces after SSRT. Cracks were observed on all the examined specimens. As the horizontal direction of the images is parallel to the elongation direction, the cracks were preferentially formed perpendicular to the elongation axis. In addition, uniform corrosion films consisting of fine grains less than 1 μm were formed on the entire specimen surface, while many particulate corrosion

deposits were randomly distributed on the surface.

The uniform corrosion films and particulate deposits on the tensile specimen after SSRT and the coupon specimen immersed in the swollen bentonite were examined using Raman spectroscopy, and the obtained spectra are presented in Figs. 3 (a)~(c), respectively. Two peaks appearing in the three spectra were identified as Cu_2O, because the doublet peak at 625 cm^{-1} accompanying the shoulder at 525 cm^{-1} is derived from Cu_2O, as reported by Chan *et al.* [12]. The three peaks observed in the spectra shown in Fig.3(b) correspond to three Raman peaks at 621.4, 339.8 and 295.4 cm^{-1}, which were identified as CuO in another study by Xu *et al.* [13]. Furthermore, Smith *et al.* reported that Cu_2S exhibited peaks at 611, 328, and 294 cm^{-1} [14]. According to the literature, we identified that the uniform corrosion film mainly consists of Cu_2O, while the particulate deposits are composed of CuO or Cu_2S. It is difficult to distinguish CuO and Cu_2S by Raman spectroscopy. EDX analysis (described later) indicated S detection for the uniform corrosion films, in contrast to the particulate deposits. Therefore, we concluded that the particulate deposits consisted of CuO. Similar spectra were obtained for both the uniform corrosion films and also the particulate deposits, regardless of the swelling solution, indicating that NH_3 does not affect the corrosion products compositions. The corrosion film on the coupon specimen immersed in a deionized water swollen bentonite at 323 K for 4 days are also mainly composed of Cu_2O, as shown in Fig.3(c).

3.2 Cross sectional characterization

The central part of the gauge section surface of the tensile specimens after SSRT was cut along the tensile axis and then mounted in an epoxy resin for SEM observation. Figures 4 (a)~(c) show cross-sectional SEM images of the tensile specimens exhibiting SCC cracks, corresponding to the specimens shown in Figs.2 (a)~(c). As apparent from the images, the cracks propagated perpendicular to the specimen surface. It is noticeable that the crack is surrounded by a phase exhibiting a different contrast from the bulk of the copper specimen. A different phase that continues to the surface layer of the cross section was identified as the surface oxide layer, as confirmed by EDX observation described

later. Figure 4 (d) shows the cross-section of the coupon specimen surface that was immersed in a pure water swollen bentonite at 323 K for 7 days, indicating that the surface oxide layer was very thin [8] compared to that formed on the tensile specimens after SSRT.

In order to gain an insight into the crack propagation mechanism, the elemental distribution near the crack was examined. Figure 5 shows EDX elemental maps obtained for the cross-section of the copper specimen after SSRT. Oxygen was distributed in the uniform corrosion film as well as the particulate deposits, while sulfur was contained mainly in the uniform corrosion film, especially underneath the particulate deposits near the crack. Therefore, it was confirmed that the phase of the surface layer continuing to the layer surrounding the SCC crack was cuprous oxide (Cu_2O), including sulfide, whereas particulate deposits over the cracks were cupric oxide (CuO).

3.3 Distribution of crack depth

In order to compare the SCC susceptibility of copper in different environments, the distribution of the number and depth of cracks were analyzed. The cross section of the specimen surface was carefully observed for 1 mm, measuring the depth of each crack. Figure 6 shows the histograms presenting the distribution of crack depth per unit length (1 mm) in gauge sections of the tensile specimens after SSRT in bentonite swollen with pure water and NH_3 aqueous solutions. The number *n* in each histogram indicated the total number of cracks observed along a 1 mm line parallel to the tensile axis for each specimen. The maximum frequency appeared at a depth of 1.5 μm, and then the frequency decreased with increasing depth for each specimen. It is noted that the distribution shifted towards a larger depth with the addition of NH_3 in the swelling water, although the number of cracks per unit length was not necessarily affected by NH_3.

4 DISCUSSION

In the present study, it was revealed that pure copper suffers from tarnish rupture type

SCC in swollen bentonite, regardless of the NH_3 content in the bentonite. This means that NH_3 is not essential for the SCC of copper in this environment, although NH_3 has historically been recognized as one of the important environmental factors that cause SCC of copper. Thus, the environment in bentonite induces SCC of pure copper. In a previous study, we reported that a uniform film comprising oxide and sulfide of copper grows in swollen bentonite [10]. For example, the thickness of the film formed at 323 K for 10 days was approximately 50 nm. However, the uniform corrosion films formed on the tensile specimen after SSRT were more than 500 nm thick as shown in Figs. 4(a)-(c). In addition, cracks were surrounded by the same corrosion products, which entirely cover the surface as a cuprous oxide film. It is considered that under plastic deformation, copper forms a relatively thick oxide/sulfide film, often broken by the tensile stress to initiate SCC crack. Further repetition of thick oxide/sulfide film formation and its breakdown results in the typical tarnish crack type SCC. To the best of our knowledge, this is the first report of tarnish crack type SCC occuring on pure copper in a swollen bentonite without NH_3, although the tarnish rupture type SCC of copper has been reported in various environments [15,16].

The surface oxide/sulfide film mainly consisted of Cu_2O, which was relatively compact compared to the CuO. In contrast, the particulate deposits distributed randomly on the tensile specimen surface were porous and confirmed to be composed of CuO. The local breakdown of the compact Cu_2O layer exposed the substrate copper to the environment, resulting in the rapid dissolution of cupric ions to form particulate CuO before a relatively protective Cu_2O layer was formed. Therefore, such particulate CuO deposits formed randomly at the sites where uniform corrosion films were locally broken by the plastic deformation, regardless of the SCC occurrence. Suzuki *et al.* reported that the SCC of copper occurred when an adherent corrosion film formed, while the SCC susceptibility was lowered with a loosely adhered corrosion film [16]. Thus, if the corrosion film is compact and rigidly adheres to the copper surface, the film is easily ruptured under loading, because the film is not able to follow the elongation of the substrate copper. The rupture causes a crack in the corrosion film, resulting in the

formation of a corrosion film underneath the crack. Repeated rupture and formation of a corrosion film lead to crack propagation by the tarnish rupture mechanism. A schematic drawing illustrating the process of tarnish crack type SCC of copper observed in swollen bentonite is depicted in Fig.7.

In aqueous solution, NH_3 attracts protons according to the following reaction:

$$NH_3 + H_2O \rightarrow NH_4^+ + OH^- \quad (1)$$

Increase in the OH^- concentration increases pH of the aqueous solution, as indicated by eq. (1). This alkalization could occur in the swollen bentonite suppressing the formation of copper sulfide [10]. The suppression of sulfide formation could retain the corrosion film compactness as shown in Fig.2. In other words, the corrosion film is found to adhere tightly to the copper substrate, which may promote the tarnish rapture as described above. Therefore, it is concluded that the addition of NH_3 enhanced the crack propagation.

5 CONCLUSION

In the present study, the SCC of pure copper was examined using SSRT in bentonite swollen with pure water containing various concentrations of NH_3. During SSRT, thick and relatively compact Cu_2O / sulfide films were formed. Local breakdown of the film induced a tarnish rupture type SCC. Rapid dissolution of cupric ions after the film breakdown resulted in the CuO formation, which covered the sites of film breakdown as porous particulate deposits. The distribution of crack depth revealed that NH_3 contained in the swollen bentonite did not necessarily increase the frequency of SCC cracks, but clearly enhanced the crack propagation rate. It is worth noting that the thickness of the oxide film formed on elongated copper was considerably larger than that formed on copper without plastic deformation in the swollen bentonite. Therefore, the synergistic effects of tensile strain and the environment provided by bentonite induce the tarnish rapture type SCC of copper.

ACKNOWLEGEMENT

This research was funded by the Secretariat of Nuclear Regulation Authority, Japan.

REFERENCES

[1] F. King, L. Ahonen, C. Taxén, U. Vuorinen, L. Werme, *Copper corrosion under expected concidtions in a deep geologic repository*, TR-01-23, Svensk Kärnbränslehantering AB, Stockholm, **2001**.

[2] Japan Nuclear Cycle Development Institute, *Engineering reliability of repository technology of high-level radioactive waste disposal in Japan*, JNC TN1400 99-022, **1999**.

[3] Japan Nuclear Cycle Development Institute, *H12: Project to Establish the Scientific and Technical Basis for HLW Disposal in Japan*, JNC TN1410 2000-003, **2000**.

[4] J. Chen, Z. Qin, D.W. Shoesmith, Kinetics of Corrosion Film Growth on Copper in Neutral Chloride Solutions Containing Small Concentrations of Sulfide, *J. Electrochem. Soc.* **2010**, 157, C338-C345.

[5] J. Chen, Z. Qin, L. Wu, J.J. Noël, D.W. Shoesmith, The influence of sulphide transport on the growth and properties of copper sulphide films on copper, *Corr. Sci.*, **2014**, 87, 233-238.

[6] T. Martino, R. Partovi-Nia, J. Chen. Z. Qin, D.W. Shoesmith, Mechanism of Film Growth on Copper in Aqueous Solutions Containing Sulphide and Chloride under Voltammetric Conditions, *Electrochim. Acta* **2014**, 127, 439-447.

[7] J. Smith, Z. Qin, F. King, L. Werme, D.W. Shoesmith, Sulfide Film Formation on Copper Under Electrochemical and Natural Corrosion Conditions, *Corrosion* **2007**, 63, 135-144.

[8] B. Rosborg, T. Kosec, A. Kranjc, J. Pan, A. Legat, Electrochemical impedance spectroscopy of pure copper exposed in bentonite under oxic conditions, *Electrochim. Acta* **2011**, 56, 7862-7870.

[9] T. Kosec, Z. Qin, J. Chen, A. Legat, D.W. Shoesmith, Copper corrosion in bentonite/saline groundwater solution: Effects of solution and bentonite chemistry, *Corr. Sci.* **2015**, 90, 248-258.

[10] S. Fujimoto and H. Tsuchiya, Oxide and Sulfide Films Formation on Copper under Simulated Disposal Environment, presented at *5th International Workshop on Long-Term Prediction of Corrosion Damage in Nuclear Waste Systems (LTC2013)*, Asahikawa, Japan 7-11 October, **2013**.

[11] N. Taniguchi, M. Kawasaki, Influence of sulfide concentration on the corrosion behavior of pure copper in synthetic seawater, *J. Nucl. Mater.* **2008**, 379, 154-161.

[12] H.Y.H. Chan, C.G. Takoudis, M.J. Weaver, Oxide Film Formation and Oxygen Adsorption on Copper in Aqueous Media As Probed by Surface-Enhanced Raman Spectroscopy, J. *Phys. Chem.* **1999**, B 103, 357-365.

[13] C. Xu, Y. Liu, G. Xu, G. Wang, Preparation and characterization of CuO nanorods by thermal decomposition of CuC_2O_4 precursor, *Mater. Res. Bull.* **2002**, 37, 2365-2372.

[14] J.M. Smith, J.C. Wren, M. Odziemkowski, D.W. Shoesmith, The Electrochemical Response of Preoxidized Copper in Aqueous Sulfide Solutions, *J. Electrochem. Soc.* **2007**, 154, C431-C438.

[15] H. Uchida, S. Inoue, M. Koyama, M. Mori, K. Koterazawa, Susceptibility to stress corrosion cracking of pure copper in $NaNO_2$ solutions, *Zairyo /J. Soc. Mater. Sci. Jpn.* **1991**, 40, 1073-1078.

[16] Y. Suzuki, Y. Hisamatsu, Stress Corrosion Cracking of Pure Copper in Dilute Ammoniacal Solutions, *Corr. Sci.* **1981**, 21, 353-368.

List of Captions

Figure 1 (a) Tensile specimen for SSRT, (b) Environmental cell for SSRT.

Figure 2 SEM images of surface of copper specimen after SSRT in the bentonite swelled with various solutions (a) deionized water, (b) 5 mM NH_3 and (c) 10 mM NH_3.

Figure 3 Raman spectra obtained from (a) uniform corrosion film and (b) particulate deposits after SSRT, and (c) from the coupon specimen immersed in bentonite swollen with deionized water for 4 days.

Figure 4 Cross sectional SEM images of copper specimens after SSRT in the bentonite swelled with various solutions: (a) deionized water, (b) 5 mM NH_3 and (c) 10 mM NH_3, and (d) of copper coupon specimen immersed in bentonite swollen with deionized water for 7 days.

Figure 5 EDX elemental maps measured for the cross section of the copper specimen after SSRT in bentonite swollen with deionized water; (a) SEM image, (b) copper, (c) oxygen and (d) sulfur.

Figure 6 Histograms presenting the distribution of crack depth obtained from the copper specimen after SSRT in the bentonite swelled with various solutions: (a) deionized water, (b) 5 mM NH_3 and (c) 10 mM NH_3.

Figure 7 Schematic drawing of the process of tarnish crack type SCC of Copper.

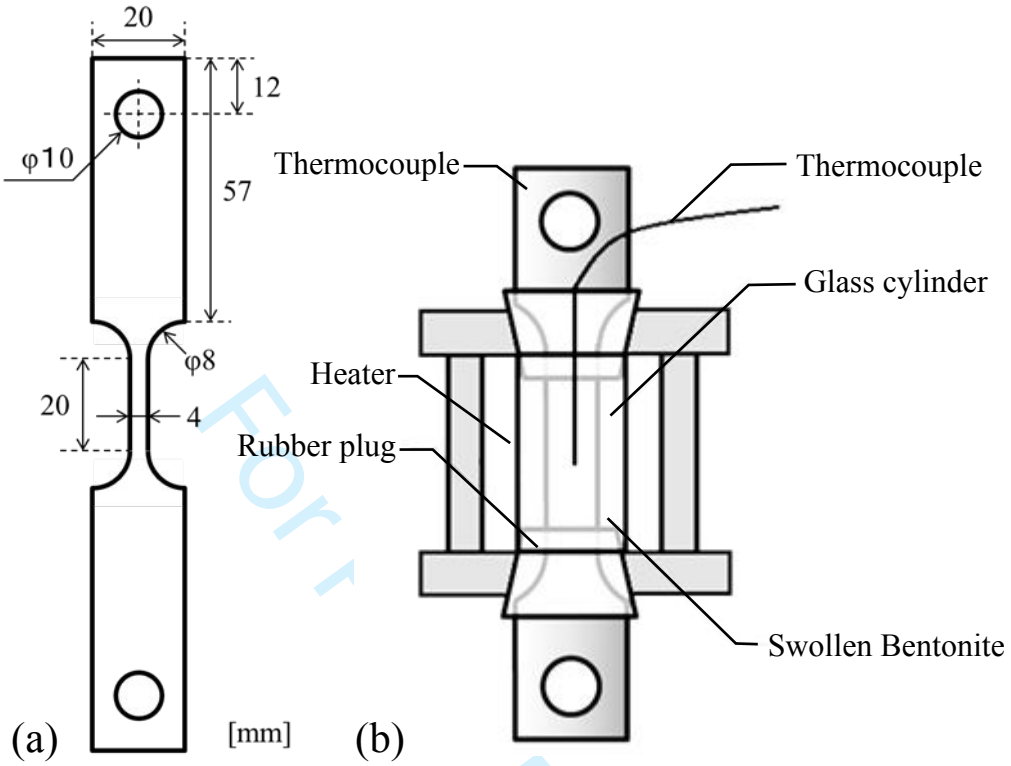

Figure 1 (a) Tensile specimen for SSRT, (b) Environmental cell for SSRT

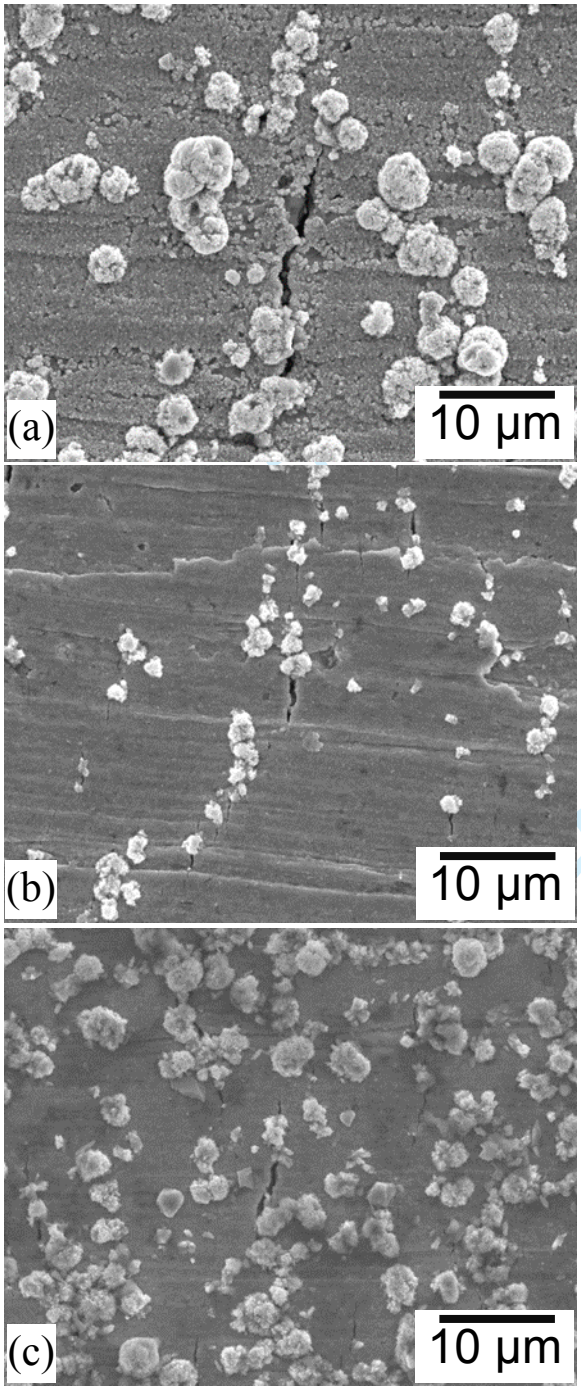

Figure 2 SEM images of surface of copper specimen after SSRT in the bentonite swelled with various solutions (a) deionized water, (b) 5 mM NH_3 and (c) 10 mM NH_3.

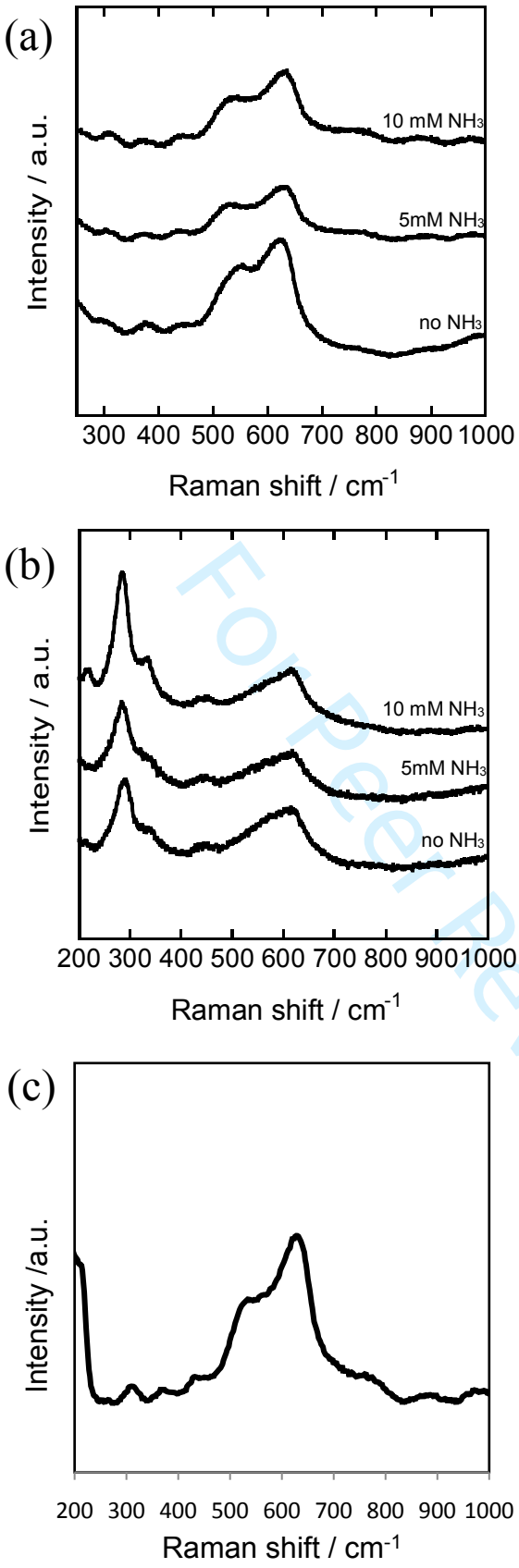

Figure 3 Raman spectra obtained from (a) uniform corrosion film and (b) particulate deposits after SSRT, and (c) from the coupon specimen immersed in bentonite swollen with deionized water for 4 days.

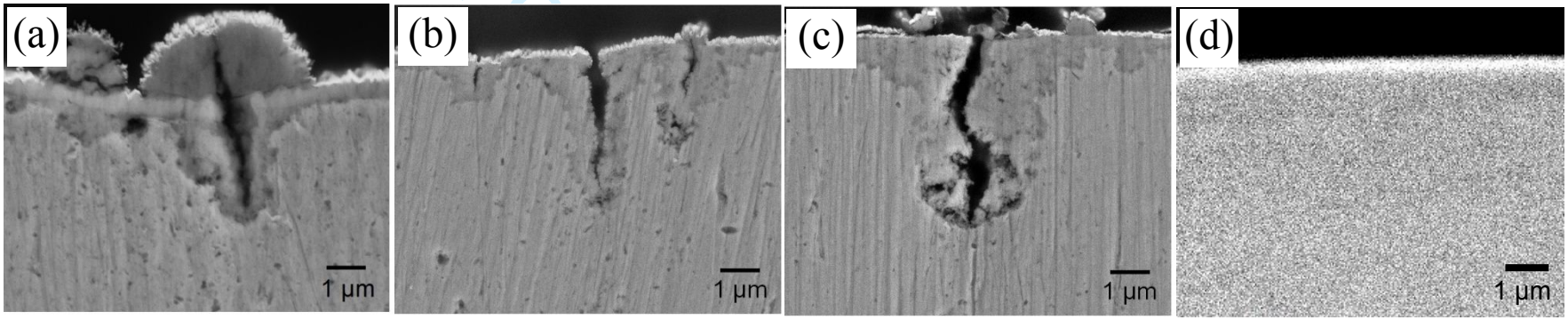

Figure 4 Cross sectional SEM images of copper specimens after SSRT in the bentonite swelled with various solutions: (a) deionized water, (b) 5 mM NH_3 and (c) 10 mM NH_3, and (d) of copper coupon specimen immersed in bentonite swollen with deionized water for 7 days.

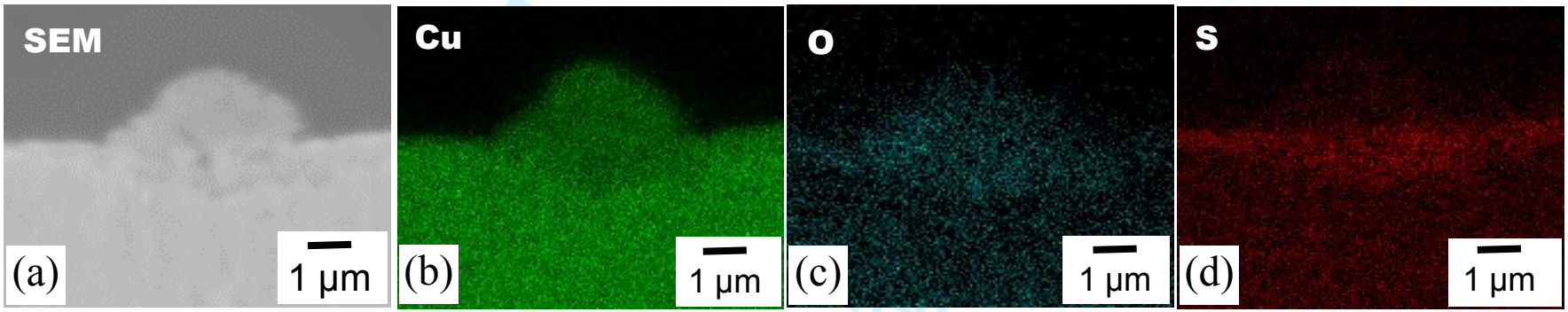

Figure 5 EDX elemental maps measured for the cross section of the copper specimen after SSRT in bentonite swollen with deionized water; (a) SEM image, (b) copper, (c) oxygen and (d) sulfur

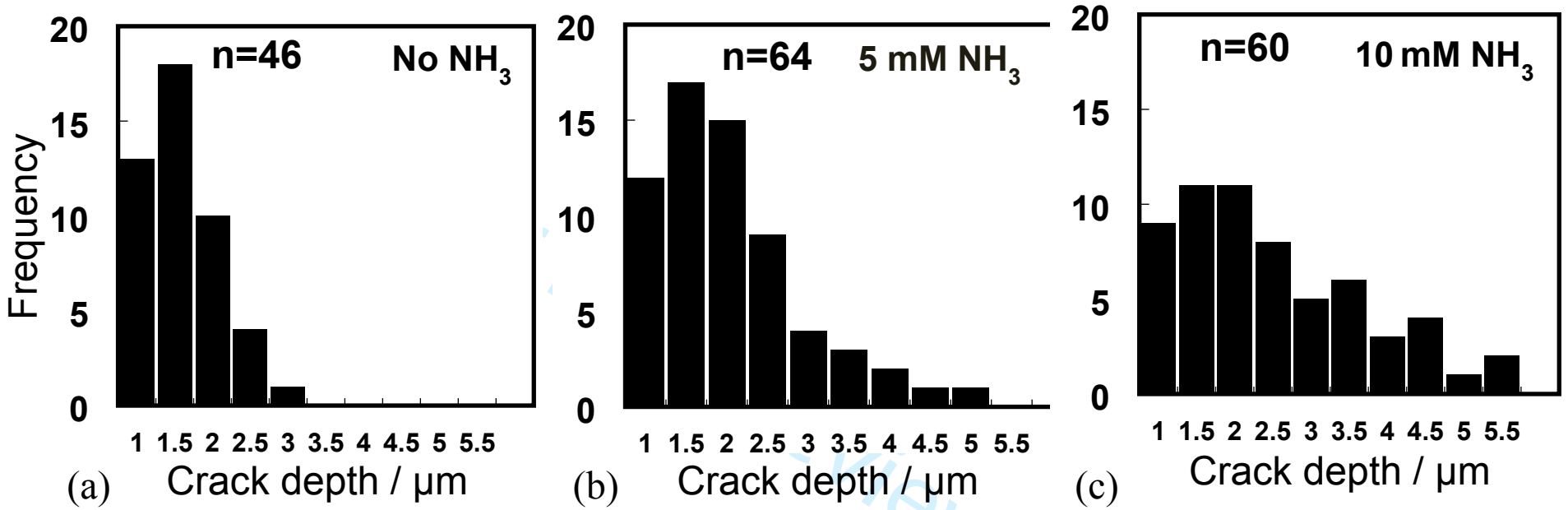

Figure 6 Histograms presenting the distribution of crack depth obtained from the copper specimen after SSRT in the bentonite swelled with various solutions: (a) deionized water, (b) 5 mM NH_3 and (c) 10 mM NH_3.

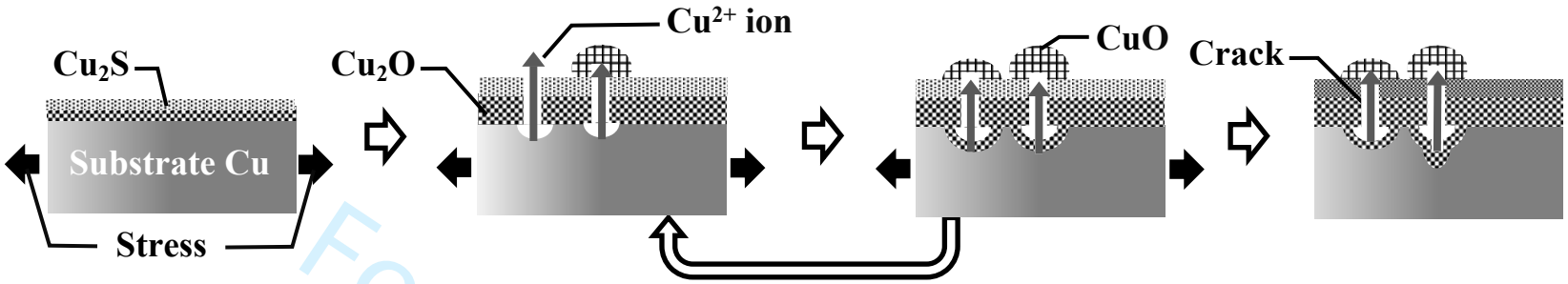

Figure 7 Schematic drawing of the process of tarnish crack type SCC of Copper